

Spin-system heterogeneities indicate a selected-fit mechanism in fatty acid binding to heart-type fatty acid-binding protein (H-FABP)

Christian LÜCKE*, Martin RADEMACHER*, Aukje W. ZIMMERMAN†, Herman T. B. VAN MOERKERK†, Jacques H. VEERKAMP† and Heinz RÜTERJANS*¹

*Institut für Biophysikalische Chemie, Johann Wolfgang Goethe-Universität, Marie-Curie-Strasse 9, 60439 Frankfurt am Main, Germany, and †Department of Biochemistry, University of Nijmegen, Geert Groteplein 30, 6525 GA Nijmegen, The Netherlands

Recent advances in the characterization of fatty acid-binding proteins (FABPs) by NMR have enabled various research groups to investigate the function of these proteins in aqueous solution. The binding of fatty acid molecules to FABPs, which proceeds through a portal region on the protein surface, is of particular interest. In the present study we have determined the three-dimensional solution structure of human heart-type FABP by multi-dimensional heteronuclear NMR spectroscopy. Subsequently, in combination with data collected on a F57S mutant we have been able to show that different fatty acids induce distinct conformational states of the protein backbone in this portal region, depending on the chain length of the fatty acid ligand.

This indicates that during the binding process the protein accommodates the ligand molecule by a 'selected-fit' mechanism. In fact, this behaviour appears to be especially pronounced in the heart-type FABP, possibly due to a more rigid backbone structure compared with other FABPs, as suggested by recent NMR relaxation studies. Thus differences in the dynamic behaviours of these proteins may be the key to understanding the variations in ligand affinity and specificity within the FABP family.

Key words: NMR spectroscopy, protein dynamics, protein–ligand interactions, selected-fit binding mechanism, solution structure.

INTRODUCTION

The family of fatty acid-binding proteins (FABPs) comprises a relatively large number of cytosolic 14–15 kDa proteins, which have been classified based on their occurrence in various tissues, such as for example heart-type FABP (H-FABP), liver-type FABP (L-FABP), intestinal-type FABP (I-FABP), brain-type FABP ('B-FABP'), epidermal-type FABP (E-FABP) or adipocyte-type FABP (A-FABP) [1,2]. Even though these proteins display different ligand-binding affinities and specificities, they are characterized by a common three-dimensional fold [3]. In general, as first described for I-FABP in a X-ray study by Sacchettini et al. [4], the fatty acid ligand is bound inside the protein body, which consists of 10 anti-parallel β -strands that form a β -clam-type structure encompassing an internal cavity. In addition a short helix-turn-helix motif closes the β -clam on one side. Subsequently, similar structural arrangements were also found for several other FABPs, e.g. human H-FABP, A-FABP, L-FABP and E-FABP [5–8].

Several studies have been aimed at understanding the molecular mechanisms that determine the differences in ligand binding observed throughout the FABP family. H-FABP, for example, was shown to display a preference for unsaturated fatty acids, especially those with chain lengths of 18 carbon atoms [9]. The fatty acid dissociation constants (K_d) have been studied for most FABP types with at least two different methods of analysis. Interestingly, the K_d values obtained by the Lipidex separation method [10–12] are generally higher (up to 100-fold) compared with those determined using the ADIFAB (acrylodan-labelled I-

FABP) fluorescent-probe technique [13,14]. Nevertheless, independently of the method used, the K_d values of H-FABP appeared to be lowest for most fatty acids of all the FABP types investigated, suggesting a particularly tight binding to the H-FABP. This is supported further by the low fatty acid-dissociation rates observed for H-FABP compared with I-FABP and A-FABP [15].

The first FABP structure determined in solution by NMR spectroscopy was that of bovine H-FABP [16]. During the course of the ¹H and ¹⁵N resonance assignments, very pronounced spin-system heterogeneities were observed [17]. By then, the source of these multiple proton spin-systems was not fully understood. The majority of the heterogeneities had been found in the so-called portal region, where the fatty acid ligand supposedly enters and exits the protein molecule [18], suggesting several subtle but distinct conformational states in this region.

The question remained, however, of whether these spin-system heterogeneities are due to different spatial orientations of the Phe-57 ring, as suggested by crystallographic studies on H-FABP [19,20], I-FABP [21] and A-FABP [22] in the presence of different ligand populations, or whether they represent different conformational states of the protein backbone, as recently proposed for E-FABP [8] on account of rather weak electron density in the loop connecting β -strands C and D. Here we show unambiguously that different fatty acids induce distinct conformational states of the protein backbone in the portal region of H-FABP. Furthermore, the backbone dynamics of H-FABP around this portal region suggest a more rigid protein structure and thus tighter binding of the fatty acid ligand compared with other FABP types.

Abbreviations used: FABP, fatty acid-binding protein; I-FABP, intestinal-type FABP; A-FABP, adipocyte-type FABP; E-FABP, epidermal-type FABP; H-FABP, heart-type FABP; L-FABP, liver-type FABP; HSQC, heteronuclear single-quantum coherence; NOE, nuclear Overhauser effect; NOESY, nuclear Overhauser enhancement and exchange spectroscopy; TOCSY, total correlation spectroscopy.

¹ To whom correspondence should be addressed (e-mail hrue@bpc.uni-frankfurt.de).

The co-ordinates of the human H-FABP have been deposited at the RCSB Protein Data Bank under the PDB accession code 1G5W.

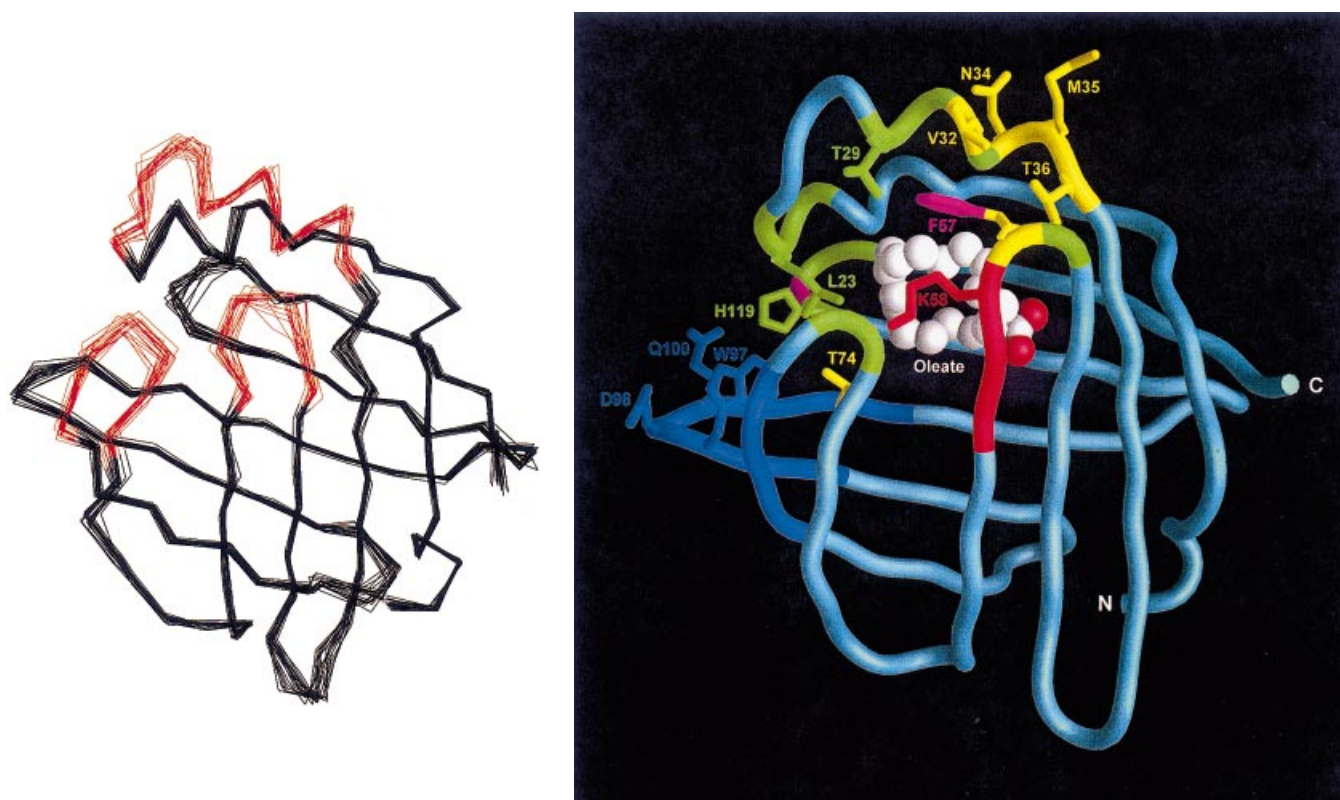


Figure 1 Three-dimensional structure of human H-FABP

Left-hand panel: solution structure ensemble representing 20 conformers of human H-FABP after energy minimization. The structural statistics are given in Table 1. An increased backbone deviation is observed for residues in the portal region (α traces shown in red), which is similar to bovine H-FABP and other FABPs [16,34–36]. Right-hand panel: graphical representation of the occurrence of multiple spin systems in native bovine H-FABP. Proton heterogeneities in the backbone (worm) and side chains (rods with amino acid labels) are treated separately, but by the same colour code. Red, yellow and green protein elements represent 4, 3 and 2 spin-system heterogeneities, respectively. Structure elements in magenta indicate smeared (Gly-120 backbone) or missing (Phe-57 ring) proton resonances. Differences in the proton resonances between the pI 5.1 and pI 4.9 isoforms are represented in dark blue. The fatty acid ligand is shown here as a space-filling model by using the X-ray structure coordinates of the oleate complex (PDB accession code 1HMS) [20]. Produced using GRASP [44].

EXPERIMENTAL

NMR sample preparation

The isolation of native bovine H-FABP was achieved according to the method of Jagschies et al. [23]. The expression and purification of recombinant bovine and human H-FABP were performed as described previously [16,24]. To obtain ^{15}N -enriched human H-FABP, the protein was expressed in M9 minimal medium with $^{15}\text{NH}_4\text{Cl}$ (Cambridge Isotope Laboratories, Andover, MA, U.S.A.) as the sole nitrogen source.

For the delipidation of the protein samples, bound bacterial fatty acids were removed by affinity chromatography at 37 °C. A Lipidex 5000 column (5 cm \times 12 cm; Canberra-Packard, Groningen, The Netherlands) was used at a slow flow rate (0.5 ml/min; 20 mM KH_2PO_4 /0.05% NaN_3 , pH 7.4) based on the delipidation procedure described by Glatz and Veerkamp [25]. For each run, 30–40 mg of protein was applied to the column. In general, the delipidation procedure was carried out twice, and the column was regenerated with methanol after each step. The protein recovery was about 65% for each run. The degree of delipidation varied between 50–80%, as determined by GC analysis [26].

The proteins were relipidated overnight at 37 °C with a 1–5-fold excess of palmitic acid ($\text{C}_{16:0}$), palmitoleic acid ($\text{C}_{16:1}$),

stearic acid ($\text{C}_{18:0}$) or oleic acid ($\text{C}_{18:1}$), depending on the solubility of the respective fatty acid in aqueous solution.

NMR experiments

All NMR measurements were performed at 37 °C on a DMX600 spectrometer operating at a ^1H resonance frequency of 600.13 MHz using a 5 mm triple-resonance ($^1\text{H}/^{13}\text{C}/^{15}\text{N}$) probe with XYZ-gradient capability (Bruker Instruments). The 1–3 mM protein samples contained purified H-FABP in a buffer solution consisting of 20 mM KH_2PO_4 , 0.05% NaN_3 and 10% $^2\text{H}_2\text{O}$ (pH 5.5). The sequence-specific ^1H and ^{15}N assignments were determined from homonuclear two-dimensional [total correlation spectroscopy (TOCSY) and nuclear Overhauser enhancement and exchange spectroscopy (NOESY)] and ^{15}N -edited multi-dimensional [heteronuclear single-quantum coherence (HSQC), heteronuclear triple-quantum coherence ('HTQC') TOCSY-HSQC and NOESY-HSQC] spectra, using the classical assignment strategy through nuclear Overhauser effect (NOE) connectivities [27]. The TOCSY experiments were performed with spinlock times of either 80 or 5 ms (to obtain COSY-type information with less spectral overlap). For the NOESY experiments mixing times between 150 and 200 ms were used. The homonuclear TOCSY and NOESY spectra were

recorded in a phase-sensitive mode with time-proportional phase incrementation of the initial pulse. Quadrature detection was used in both dimensions with the carrier placed in the centre of the spectrum on the water resonance. The water signal was suppressed by selective presaturation during the relaxation delay. In the NOESY experiments water saturation was applied also during the mixing time. All three-dimensional experiments made use of pulsed-field gradients for coherence selection and artifact suppression, and utilized gradient sensitivity-enhancement schemes wherever appropriate [28]. Quadrature detection in the indirectly-detected dimensions was obtained by either the States/TPPI (time-proportional phase incrementation) or the echo/anti-echo methods. Baseline corrections were applied wherever necessary. Experimental evidence about hydrogen bonds was obtained from proton/deuterium exchange. All spectra were calibrated with respect to 2,2-dimethyl-2-silapentane-5-sulphonate (Cambridge Isotope Laboratories) as an external reference [29].

Data processing and analysis

The spectral data were processed on a Silicon Graphics Indy workstation using the Bruker XWIN-NMR 1.3 software package. Peak-picking and data analysis of the transformed spectra were performed using the AURELIA 2.5.9 program (Bruker).

The NOE-derived distance restraints were determined from two-dimensional homonuclear NOESY and three-dimensional ^{15}N -edited NOESY-HSQC spectra. The cross-peak intensities were grouped into different distance categories of 2.5, 3.5, 4.5 and 6.0 Å. Assignments of ambiguous NOE cross-peaks were made by applying a structure-aided filtering strategy in repeated rounds of structure calculations using the DYANA 1.5 program package [30]. Starting *ab initio*, 100 conformers were finally calculated by DYANA in 8000 annealing steps each. Subsequent energy minimization in the presence of the NMR restraints, carried out with the DISCOVER module of the INSIGHT 97 software package (Molecular Simulations, San Diego, CA, U.S.A.), was performed on the 20 best DYANA conformers using the consistent valence force field (CVFF) [31] with a dielectric constant equal to 4. The resulting structures were analysed using the PROCHECK-NMR software [32].

RESULTS AND DISCUSSION

Solution structure of human H-FABP

Based on the chemical shift values of bovine H-FABP [16], the sequence-specific ^1H and ^{15}N resonance assignments (available at <http://www.BiochemJ.org/bj/354/bj3540259add.htm>) have been determined for human H-FABP, which displays 89% sequence homology with the bovine protein [33]. Subsequently, the solution structure of human H-FABP has been obtained from NOE data. The three-dimensional fold of this protein (Figure 1, left-hand panel) is typical for all FABPs, as mentioned in the Introduction. The structural statistics of this well-defined structure ensemble after energy minimization are given in Table 1. Most notable is the increased backbone dispersion in the so-called portal region (red-coloured $\text{C}\alpha$ traces in Figure 1, left-hand panel), as also pointed out in a series of NMR studies on various FABPs [16,34–36]. Thus the backbone root-mean-square deviation value for residues 24–36, 54–59 and 73–79 (1.15 ± 0.29 Å) is on average almost 0.5 Å higher than for the rest of the protein (0.68 ± 0.08 Å; excluding the terminal residues Val-1 and Ala-132). This result indicates clearly that the above-mentioned residues of the portal region may occupy a larger conformational space compared with the non-portal residues.

Table 1 Structural statistics of the 20 selected structures of human H-FABP after energy minimization

RMSD, root-mean-square deviation.

Structural statistics	
Total number of residues	132
Total number of distance restraints	2629
Intraresidual	404
Sequential ($ i-j = 1$)	646
Medium range ($1 < i-j < 5$)	398
Long range ($ i-j > 4$)	1141
H-bonds	40
Total number of violated restraints > 0.4 Å	0
Total number of violated restraints > 0.3 Å	1
Total number of violated restraints > 0.2 Å	15
Maximal restraint violation (Å)	0.34
Ramachandran plot statistics	
Residues in most favoured regions (%)	81.8
Residues in additionally allowed regions (%)	16.2
Residues in generously allowed regions (%)	1.2
Residues in disallowed regions (%)	0.9
Structural precision (residues 2–131)	
RMSD for the backbone atoms (Å)	Ensemble 0.83 ± 0.12
RMSD for the heavy atoms (Å)	1.28 ± 0.12
Structural precision (residues 2–23, 37–53, 60–72, 80–131)	
RMSD for the backbone atoms (Å)	Ensemble 0.68 ± 0.08
RMSD for the heavy atoms (Å)	1.10 ± 0.09
Structural precision (residues 24–36, 54–59, 73–79)	
RMSD for the backbone atoms (Å)	Ensemble 1.15 ± 0.29
RMSD for the heavy atoms (Å)	1.78 ± 0.34

Table 2 Residues displaying multiple proton resonances in either the backbone or side chains of native bovine H-FABP

Only cases with significant changes in the chemical shift values (> 0.03 p.p.m.) have been chosen. N.A., not applicable.

Residue	Number of multiple proton resonances	
	Backbone	Side chain
Lys-21	2	—
Ser-22	2	—
Leu-23	2	2
Gly-24	2	N.A.
Thr-29	2	2
Arg-30	2	—
Gln-31	2	—
Val-32	3	3
Gly-33	2	N.A.
Asn-34	3	3
Met-35	3	3
Thr-36	3	3
Thr-56	2	—
Phe-57	3	3
Lys-58	4	4
Asn-59	4	—
Thr-60	4	—
Thr-74	—	3
Ala-75	2	—
Asp-76	2	—
His-119	2	2
Thr-121	2	—
Ala-122	2	—

Spin-system heterogeneities

In a previous study on native bovine H-FABP proton spin-system heterogeneities were observed for various amino acid residues [17]. It was shown that these multiple spin-systems

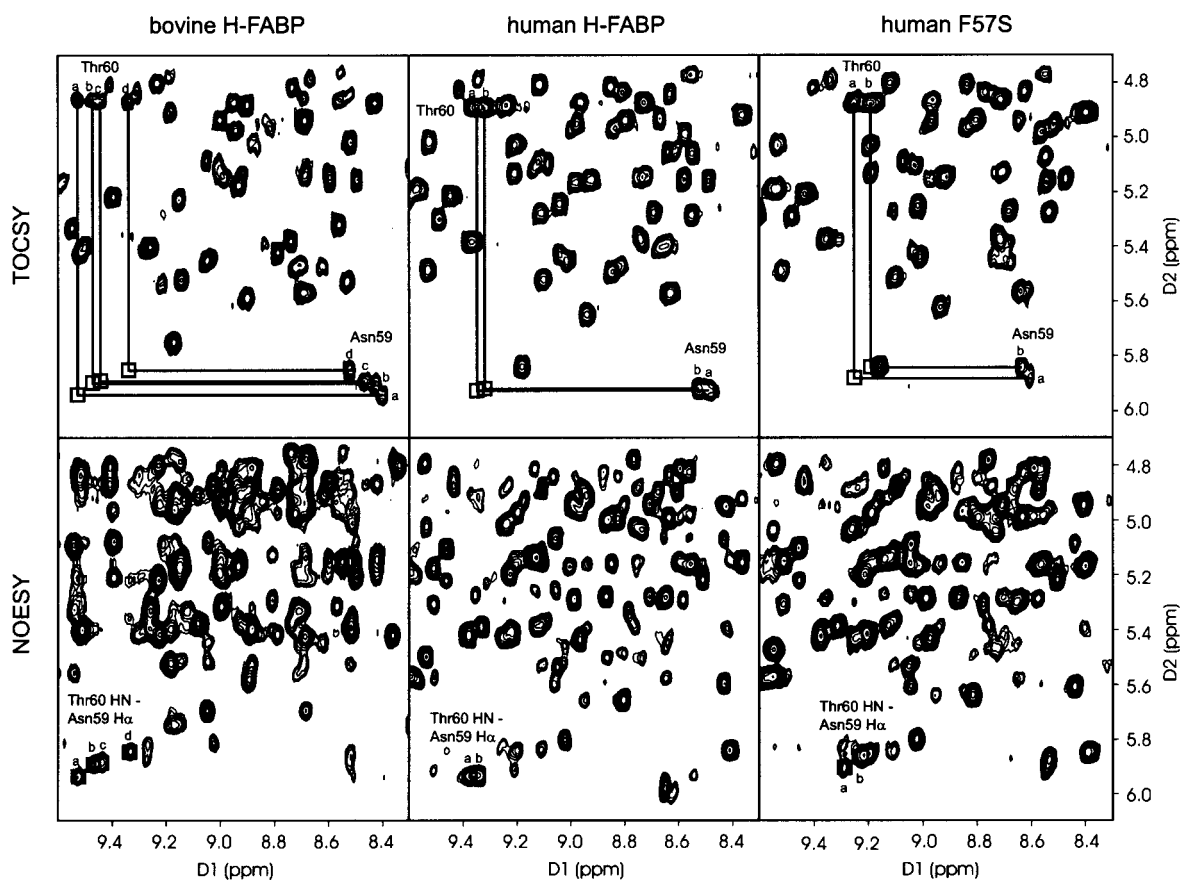


Figure 2 Part of the fingerprint regions in the TOCSY (upper panels) and NOESY (lower panels) spectra of native bovine H-FABP (left-hand panels), recombinant human H-FABP (centre panels) and the F57S mutant of recombinant human H-FABP (right-hand panels)

The TOCSY spectrum shows multiple HN-C α H correlations, representing heterogeneities of the proton resonance spin systems, for both Asn-59 and Thr-60. In the NOESY spectrum, each of these spin systems is correlated only with the respective spin system of the corresponding conformational state. In the case of the bovine H-FABP four separate proton spin systems (a–d) are observed, while for recombinant human H-FABP and the human F57S mutant protein only two such spin systems (a and b) can be distinguished for both Asn-59 and Thr-60. The differences in chemical shift values between the latter two proteins are due to the F57S mutation nearby.

represent several different but stable conformational states, which do not exchange within the NOESY time frame of 100–200 ms. Table 2 lists all residues of bovine H-FABP that show more than one set of proton resonances. For a better overview of the spatial relationships of these particular residues, the same information is shown in Figure 1 (right-hand panel). It is quite obvious that the region where these heterogeneities mainly occur is centred between helix α II and the turns connecting β -strands C and D as well as E and F. This corresponds to the above-mentioned portal region, the only opening in the protein surface through which the fatty acid apparently can enter and exit the internal binding cavity [18].

The heterogeneities in the portal region are most prominent for Lys-58, Asn-59 and Thr-60, where each residue displays four different proton resonances for both the backbone amide and the C α proton. Thus for each of these residues four separate cross-peaks representing the HN-C α H correlation can be observed in the TOCSY spectrum, as shown in the case of Asn-59 and Thr-60 in Figure 2 (upper left panel). Furthermore, in the NOESY spectrum each proton spin system of Asn-59 displays only a single sequential $d_{\alpha\alpha}(i,i+1)$ NOE connectivity to the corresponding spin system of Thr-60 (Figure 2, lower left panel).

The same effect can be observed in the ^{15}N -edited spectra of isotopically enriched H-FABP. A section from the ^{15}N -HSQC

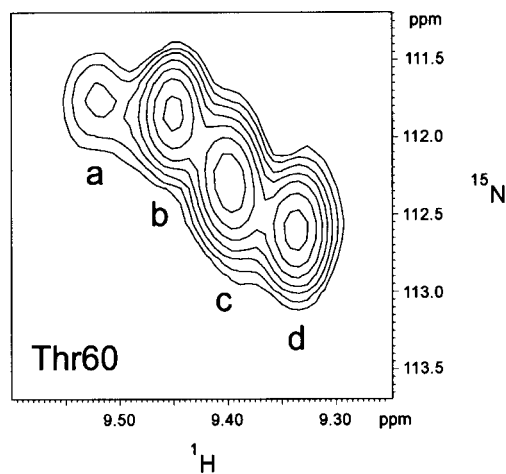


Figure 3 Part of the ^{15}N -HSQC spectrum of bovine H-FABP showing the four separate backbone amide signals that belong to the multiple spin systems of Thr-60

The signal intensities are not directly comparable with the homonuclear spectra shown in Figure 2, since a different protein sample was used (see under 'Fatty acid ligands').

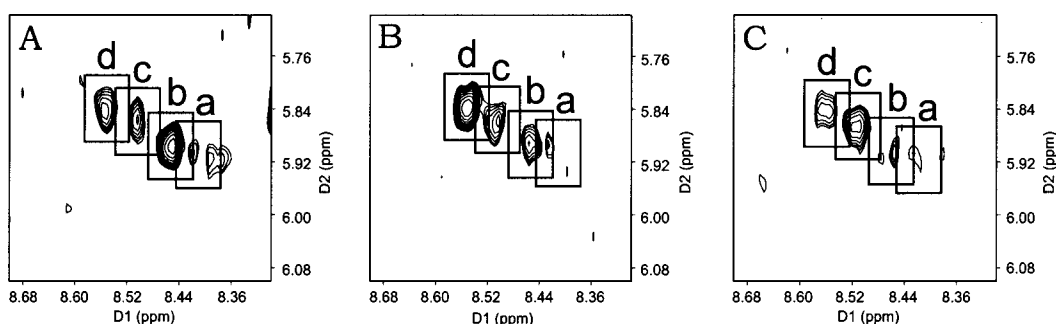


Figure 4 Close-up of the TOCSY region showing the spin-system heterogeneities for Asn-59 in three different delipidated samples (A, B and C) of recombinant bovine H-FABP

The intensity fluctuations in these spectra indicate that none of the four conformational states uniquely predominates in the apo-protein, which represents about 80% of the combined peak volume in each case.

spectrum of bovine H-FABP, representing the four separate spin systems of Thr-60, is shown in Figure 3. Moreover, for each residue with multiple spin systems, the separate backbone amide signals all display comparable dynamic behaviour, as determined by ^{15}N relaxation experiments (C. Lücke, unpublished work).

A second region in native bovine H-FABP, where multiple resonance assignments have been observed, is located around residue 98 (Figure 1, right-hand panel). This is due to the presence of a second protein isoform (pI 4.9), where Asn-98 is replaced by Asp-98 [23]. However, this effect is absent in the recombinant protein, where the pI 5.1 isoform of bovine H-FABP prevails [37].

The source of the spin-system heterogeneities in the portal region was not fully understood at first. Subtle conformational differences, as also suggested by Lu et al. [38] in the case of cellular retinol-binding protein type II (CRBP II), appeared to be the most feasible explanation. Several X-ray studies on different FABP types, including H-FABP, have reported variable positioning of the Phe-57 ring in different lipidation states, implying a dependence of the Phe-57 side-chain orientation on the fatty acid chain length [19–22]. Since Phe-57 is highly conserved throughout the family of FABPs, its phenyl ring has been suggested to play a role at the ligand entry site of these proteins as an adjustable lid covering the portal [21]. In NMR spectra, changing orientations of an aromatic ring may cause shifts in the resonance frequencies of neighbouring nuclei due to the so-called 'ring-current effect'. Thus the different states observed for H-FABP on account of varying chemical shift values could be accounted for by distinct orientations of the Phe-57 ring. As shown in the following section, however, that is not the case. Even though the Phe-57 ring may very well be free to adopt different conformations, this is not the cause for the observed spin-system heterogeneities.

Human H-FABP

In analogy to the bovine protein, spin-system heterogeneities were also observed for the human homologue. In Figure 2 (centre panels) these multiple spin systems of human H-FABP are again shown in the case of residues Asn-59 and Thr-60. Even though the number of separated spin systems is less than for bovine H-FABP, the presence of multiple conformational states is nevertheless apparent for human H-FABP as well.

In order to rule out the ring-current effect of Phe-57 as the possible cause for the observed spin-system heterogeneities, we

employed a F57S mutant of human H-FABP. The mutation of Phe-57 to Ser-57 had no significant effect on the binding affinity for oleic acid relative to the wild-type protein [39], which stands in contrast with the results reported for the analogous mutants of A-FABP and I-FABP [40,41]. In the NMR spectra the F57S mutant shows chemical shift values almost identical to the wild-type protein, except for protons located in the immediate vicinity of residue 57, suggesting little overall conformational change due to the mutation. Multiple spin systems in the portal region, however, are observed in this mutant as well (Figure 2, right-hand panels). Therefore, a changing ring-current effect, which induces shifts in neighbouring proton resonances due to different orientations of the Phe-57 side chain upon ligand binding, can definitely be ruled out. In other words, the spin-system heterogeneities in fact represent distinct backbone conformations.

Fatty acid ligands

Subsequently, we have investigated the effects of different fatty acid ligands bound to H-FABP on the distribution of spin-system heterogeneities in the NMR spectra. In order to obtain H-FABP samples with homogeneous ligand populations, the protein had to be delipidated first. Using the Lipidex procedure, at best only 80% of the endogenous fatty acids could be removed (see the Experimental section). The incomplete delipidation may be caused by the relatively tight binding of the fatty acid ligands by H-FABP compared with other FABPs.

Depending on the protein preparation, different intensity relationships were observed for the HN-C α H cross-peaks of Asn-59 in the TOCSY spectra of the delipidated protein samples (Figure 4). The sum of the volumes of all four peaks corresponds to the average volume of the unique HN-C α H signals. Since only approx. 20% of each protein sample remained lipidated, as confirmed by GC analysis, it can be concluded that the 'apo-form' represents approx. 80% of the combined peak volume. Since none of the four peaks was found to be predominant in the delipidated samples, a slow exchange between all conformational states appears most likely for the apo-form of H-FABP.

Next the delipidated bovine H-FABP sample was relipidated with palmitic acid, palmitoleic acid, stearic acid or oleic acid. The TOCSY spectra of the protein complexes thus obtained clearly show (Figure 5) that each fatty acid induces a different single yet pronounced HN-C α H correlation, suggesting a preferred backbone conformational state. In the case of the four spin systems assigned to Asn-59, for example, the series of HN-C α H cross-peaks in the fingerprint region, starting from the upper left,

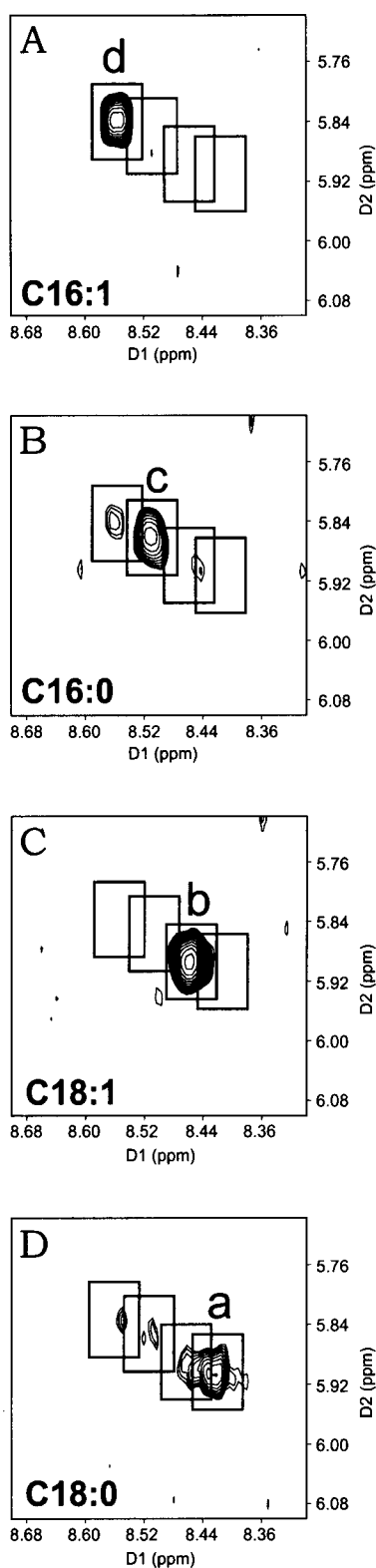


Figure 5 Close-up of the TOCSY region showing the spin-system heterogeneities for Asn-59 after relipidation of bovine H-FABP with (A) palmitoleic acid ($C_{16:1}$), (B) palmitic acid ($C_{16:0}$), (C) oleic acid ($C_{18:1}$) and (D) stearic acid ($C_{18:0}$)

These spectra show clearly that each fatty acid ligand induces a single preferred conformational state, such as state a for stearic acid, state b for oleic acid, state c for palmitic acid and state d for palmitoleic acid. (In some cases, due to different delipidation results, additional conformational states appear in the spectrum with weaker intensities.)

represent palmitoleic acid ($C_{16:1}$), palmitic acid ($C_{16:0}$), oleic acid ($C_{18:1}$) and stearic acid ($C_{18:0}$), respectively. Thus this arrangement indicates a direct dependence of the backbone conformational state on the chain length of the fatty acid ligand.

It should be noted that the incompletely delipidated samples shown in Figure 4 were subsequently relipidated with an excess of one single fatty acid, as described in the Experimental section. Thereby, most of the remaining ligand populations were displaced by the surplus of that particular fatty acid. For example, the relipidation of the previously delipidated sample shown in Figure 4(A) with excess of stearic acid ($C_{18:0}$) resulted in the spectrum shown in Figure 5(D), where oleic acid ($C_{18:1}$), palmitic acid ($C_{16:0}$) and palmitoleic acid ($C_{16:1}$), representing the conformational states b–d, have almost completely disappeared, thus leaving state a as the new predominant conformational state.

In the case of the wild-type and F57S mutant human H-FABPs, only the oleic acid complexes were prepared. Analogous to bovine H-FABP, just one single prominent HN-C α H correlation was subsequently observed in the TOCSY spectra (Figure 6), indicating a preferred backbone conformational state for the oleate complex of the human protein as well. Therefore it may be concluded that the presence of apparently only two proton spin systems in non-delipidated human H-FABP is due to the prevalence of just two different bound fatty acid types (apparently oleic and palmitic acid) in these recombinantly expressed protein samples.

NMR relaxation studies by various groups have revealed significant dynamic differences between several FABPs, suggesting a direct correlation between the dynamic and ligand-binding properties of these proteins [34]. Especially the ^{15}N relaxation studies showed major differences in the dynamic behaviour of the protein backbone between A-FABP and H-FABP, between H-FABP and ileal lipid-binding protein, as well as between I-FABP in the apo and holo forms [36,42,43]. In all these studies H-FABP appears to display the most rigid backbone structure of all FABP types, based on the mobilities determined for the picosecond-to-nanosecond (S^2) as well as microsecond-to-millisecond (R_{ex}) time scales. Even in the portal region the backbone dynamics parameters of those residues displaying spin-system heterogeneities in H-FABP are basically equivalent with the rest of the protein [43]. For A-FABP, I-FABP and ileal lipid-binding protein, on the other hand, higher backbone mobilities have been reported [36,42,43]. These data strongly suggest a direct correlation between fatty acid binding and protein dynamics.

In fact, the incomplete delipidation results of the Lipidex procedure for H-FABP reflect the relatively tight binding of fatty acids to this particular FABP type. In the apo form no preferred conformational state is apparent, while the holo form consists of several rigid but distinct backbone conformations that are induced by the specific fatty acid molecule bound to the protein. Thus the protein appears to bind the ligand tightly by adjusting the portal structure in a selected-fit type of mechanism.

Conclusions

The selected-fit binding in H-FABP appears not to be dependent on the presence of the Phe-57 ring, since the binding affinity is not influenced significantly by the mutation of this residue [39], which stands in contrast with the results reported for A-FABP and I-FABP [40,41]. Moreover, the E-FABPs, which bind single fatty acid molecules in an analogous manner to H-FABP, have either a leucine or valine residue in place of Phe-57 [8]. Thus even though ‘Phe-57’ may act as an adjustable lid on the entry portal, for certain FABP types such as H-FABP and E-FABP a phenyl

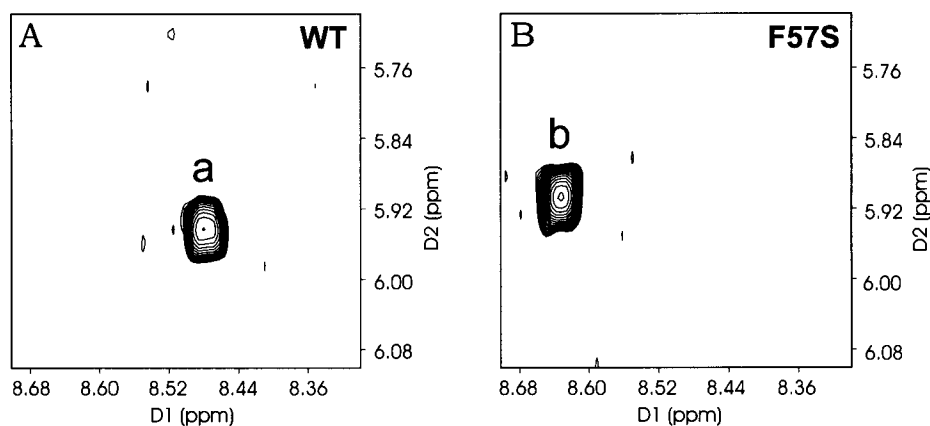


Figure 6 Close-up of the TOCSY region showing the spin-system heterogeneities for Asn-59 after relipidation of the human wild-type (WT) and F57S mutant H-FABPs with oleic acid

Clearly, in comparison with Figure 2 (upper centre and right-hand panels), only a single conformational state prevails in the oleate complexes of the wild-type protein (A, state a) and the F57S mutant (B, state b).

ring at this position of the ligand entry site does not appear to be crucial for the protein function. This conclusion is supported further by the fact that the F57S mutant of H-FABP displays the same kind of spin-system heterogeneities in the portal region as the wild-type protein, suggesting a very similar binding behaviour based on various backbone conformational states.

The correlation between backbone dynamics in the portal region and ligand-binding affinity may explain, at least in part, the functional diversity observed within the FABP family. Apparently, the fatty acid ligand, when caught inside the binding cavity of H-FABP by the selected-fit binding mechanism, will not be released from this relatively rigid protein structure as easily as from other FABPs, as shown previously by the data of Richieri et al. [15]. These differences in dissociation rates could therefore possibly reflect the specific role that each FABP type plays in its respective physiological environment.

We thank Professor M. Schubert-Zsilavecz and co-workers (Institut für Pharmazeutische Chemie, University of Frankfurt, Frankfurt, Germany) for the GC analyses. The European Large Scale Facility for Biomolecular NMR at the University of Frankfurt is kindly acknowledged for the use of its equipment.

REFERENCES

- Veerkamp, J. H., Peeters, R. A. and Maatman, R. G. H. J. (1991) Structural and functional features of different types of cytoplasmic fatty acid-binding proteins. *Biochim. Biophys. Acta* **1081**, 1–24
- Banaszak, L., Winter, N., Xu, Z., Bernlohr, D. A., Cowan, S. and Jones, T. A. (1994) Lipid-binding proteins: a family of fatty acid and retinoid transport proteins. *Adv. Protein Chem.* **45**, 89–151
- Veerkamp, J. H. and Maatman, R. G. H. J. (1995) Cytoplasmic fatty acid-binding proteins: their structure and genes. *Progr. Lipid Res.* **34**, 17–52
- Sacchettini, J. C., Gordon, J. I. and Banaszak, L. J. (1989) Crystal structure of rat intestinal fatty-acid-binding protein. *J. Mol. Biol.* **208**, 327–339
- Zanotti, G., Scapin, G., Spadon, P., Veerkamp, J. H. and Sacchettini, J. C. (1992) Three-dimensional structure of recombinant human muscle fatty acid-binding protein. *J. Biol. Chem.* **267**, 18541–18550
- Xu, Z., Bernlohr, D. A. and Banaszak, L. J. (1992) Crystal structure of recombinant murine adipocyte lipid-binding protein. *Biochemistry* **31**, 3484–3492
- Thompson, J., Winter, N., Terwey, D., Bratt, J. and Banaszak, L. (1997) The crystal structure of the liver fatty acid-binding protein. A complex with two bound oleates. *J. Biol. Chem.* **272**, 7140–7150
- Hohoff, C., Börchers, T., Rüstow, B., Spener, F. and van Tilbeurgh, H. (1999) Expression, purification, and crystal structure determination of recombinant human epidermal-type fatty acid binding protein. *Biochemistry* **38**, 12229–12239
- Maatman, R. G. H. J., van Moerkerk, H. T. B., Nooren, I. M. A., van Zoelen, E. J. J. and Veerkamp, J. H. (1994) Expression of human liver fatty acid-binding protein in *Escherichia coli* and comparative analysis of its binding characteristics with muscle fatty acid-binding protein. *Biochim. Biophys. Acta* **1214**, 1–10
- Lowe, J. B., Sacchettini, J. C., Laposata, M., McQuillan, J. J. and Gordon, J. I. (1987) Expression of rat intestinal fatty acid-binding protein in *Escherichia coli*. *J. Biol. Chem.* **262**, 5931–5937
- Paulussen, R. J. A., van der Logt, C. P. E. and Veerkamp, J. H. (1988) Characterization and binding properties of fatty acid-binding proteins from human, pig, and rat heart. *Arch. Biochem. Biophys.* **264**, 533–545
- Nemecz, G., Hubbell, T., Jefferson, J. R., Lowe, J. B. and Schroeder, F. (1991) Interaction of fatty acids with recombinant rat intestinal and liver fatty acid-binding proteins. *Arch. Biochem. Biophys.* **286**, 300–309
- Richieri, G. V., Ogata, R. T. and Kleinfeld, A. M. (1992) A fluorescently labeled intestinal fatty acid binding protein. Interactions with fatty acids and its use in monitoring free fatty acids. *J. Biol. Chem.* **267**, 23495–23501
- Richieri, G. V., Ogata, R. T. and Kleinfeld, A. M. (1994) Equilibrium constants for the binding of fatty acids with fatty acid-binding proteins from adipocyte, intestine, heart, and liver measured with the fluorescent probe ADIFAB. *J. Biol. Chem.* **269**, 23918–23930
- Richieri, G. V., Ogata, R. T. and Kleinfeld, A. M. (1996) Kinetics of fatty acid interactions with fatty acid binding proteins from adipocyte, heart, and intestine. *J. Biol. Chem.* **271**, 11291–11300
- Lassen, D., Lücke, C., Kveder, M., Mesgarzadeh, A., Schmidt, J. M., Specht, B., Lezius, A., Spener, F. and Rüterjans, H. (1995) Three-dimensional structure of bovine heart fatty-acid-binding protein with bound palmitic acid, determined by multidimensional NMR spectroscopy. *Eur. J. Biochem.* **230**, 266–280
- Lücke, C., Lassen, D., Kreienkamp, H.-J., Spener, F. and Rüterjans, H. (1992) Sequence-specific ^1H -NMR assignment and determination of the secondary structure of bovine heart fatty acid-binding protein. *Eur. J. Biochem.* **210**, 901–910
- Sacchettini, J. C., Scapin, G., Gopaul, D. and Gordon, J. I. (1992) Refinement of the structure of *Escherichia coli*-derived rat intestinal fatty acid binding protein with bound oleate to 1.75-Å resolution. *J. Biol. Chem.* **267**, 23534–23545
- Scapin, G., Young, A. C. M., Kromminga, A., Veerkamp, J. H., Gordon, J. I. and Sacchettini, J. C. (1993) High resolution X-ray studies of mammalian intestinal and muscle fatty acid-binding proteins provide an opportunity for defining the chemical nature of fatty acid:protein interactions. *Mol. Cell. Biochem.* **123**, 3–13
- Young, A. C. M., Scapin, G., Kromminga, A., Patel, S. B., Veerkamp, J. H. and Sacchettini, J. C. (1994) Structural studies on human muscle fatty acid binding protein at 1.4 Å resolution: binding interactions with three C18 fatty acids. *Structure* **2**, 523–534
- Eads, J., Sacchettini, J. C., Kromminga, A. and Gordon, J. I. (1993) *Escherichia coli*-derived rat intestinal fatty acid binding protein with bound myristate at 1.5 Å resolution and I-FABP^{Arg106→Gln} with bound oleate at 1.74 Å resolution. *J. Biol. Chem.* **268**, 26375–26385

- 22 Xu, Z., Bernlohr, D. A. and Banaszak, L. J. (1993) The adipocyte lipid-binding protein at 1.6-Å resolution. Crystal structures of the apoprotein and with bound saturated and unsaturated fatty acids. *J. Biol. Chem.* **268**, 7874–7884
- 23 Jagschies, G., Reers, M., Unterberg, C. and Spener, F. (1985) Bovine fatty acid binding proteins – isolation and characterisation of two cardiac fatty acid binding proteins that are distinct from corresponding hepatic proteins. *Eur. J. Biochem.* **152**, 537–545
- 24 Peeters, R. A., Ena, J. M. and Veerkamp, J. H. (1991) Expression in *Escherichia coli* and characterization of the fatty-acid-binding protein from human muscle. *Biochem. J.* **278**, 361–364
- 25 Glatz, J. F. C. and Veerkamp, J. H. (1983) Removal of fatty acids from serum albumin by Lipidex 1000 chromatography. *J. Biochem. Biophys. Methods* **8**, 57–61
- 26 Müller, K.-D., Husmann, H. and Nalik, H. P. (1990) A new and rapid method for the assay of bacterial fatty acids using high resolution capillary gas chromatography and trimethylsulfonium hydroxide. *Zbl. Bakt.* **274**, 174–182
- 27 Wüthrich, K. (1986) *NMR of Proteins and Nucleic Acids*, Wiley, New York
- 28 Muhandiram, D. R. and Kay, L. E. (1994) Gradient-enhanced triple-resonance three-dimensional NMR experiments with improved sensitivity. *J. Magn. Reson. Ser. B* **103**, 203–216
- 29 Wishart, D. S., Bigam, C. G., Yao, J., Abildgaard, F., Dyson, H. J., Oldfield, E., Markley, J. L. and Sykes, B. D. (1995) ^1H , ^{13}C and ^{15}N chemical shift referencing in biomolecular NMR. *J. Biomol. NMR* **6**, 135–140
- 30 Güntert, P., Mumenthaler, C. and Wüthrich, K. (1997) Torsion angle dynamics for NMR structure calculation with the new program DYANA. *J. Mol. Biol.* **273**, 283–298
- 31 Dauber-Ogusthorpe, P., Roberts, V. A., Ogusthorpe, D. J., Wolff, D. J., Genest, M. and Hagler, A. T. (1988) Structure and energetics of ligand binding to proteins: *E. coli* dihydrofolate reductase-trimethoprim, a drug-receptor system. *Proteins* **4**, 31–47
- 32 Laskowski, R. A., MacArthur, M. W., Moss, D. S. and Thornton, J. M. (1993) AQUA and PROCHECK-NMR: Programs for checking the quality of protein structures solved by NMR. *J. Appl. Crystallogr.* **26**, 283–291
- 33 Peeters, R. A., Veerkamp, J. H., Van Kessel, A. G., Kanda, T. and Ono, T. (1991) Cloning of the cDNA encoding skeletal-muscle fatty-acid-binding protein, its peptide sequence and chromosomal localization. *Biochem. J.* **276**, 203–207
- 34 Lücke, C., Zhang, F., Rüterjans, H., Hamilton, J. A. and Sacchettini, J. C. (1996) Flexibility is a likely determinant of binding in the case of ileal lipid binding protein. *Structure* **4**, 785–800
- 35 Zhang, F., Lücke, C., Baier, L. J., Sacchettini, J. C. and Hamilton, J. A. (1997) Solution structure of human intestinal fatty acid binding protein: implications for ligand entry and exit. *J. Biomol. NMR* **9**, 213–228
- 36 Hodsdon, M. E. and Cistola, D. P. (1997) Ligand binding alters the backbone mobility of intestinal fatty acid-binding protein as monitored by ^{15}N relaxation and ^1H exchange. *Biochemistry* **36**, 2278–2290
- 37 Billich, S., Wissel, T., Kratzin, H., Hahn, U., Hagenhoff, B., Lezius, A. and Spener, F. (1988) Cloning of a full-length complementary DNA for fatty-acid-binding protein from bovine heart. *Eur. J. Biochem.* **175**, 549–556
- 38 Lu, J., Lin, C.-L., Tang, C., Ponder, J. W., Kao, J. L. F., Cistola, D. P. and Li, E. (2000) Binding of retinol induces changes in rat cellular retinol-binding protein II conformation and backbone dynamics. *J. Mol. Biol.* **300**, 619–632
- 39 Prinsen, C. F. M. and Veerkamp, J. H. (1996) Fatty acid binding and conformational stability of mutants of human muscle fatty acid-binding protein. *Biochem. J.* **314**, 253–260
- 40 Simpson, M. A. and Bernlohr, D. A. (1998) Analysis of a series of phenylalanine 57 mutants of the adipocyte lipid-binding protein. *Biochemistry* **37**, 10980–10986
- 41 Richieri, G. V., Low, P. J., Ogata, R. T. and Kleinfeld, A. M. (1998) Thermodynamics of fatty acid binding to engineered mutants of the adipocyte and intestinal fatty acid binding proteins. *J. Biol. Chem.* **273**, 7397–7405
- 42 Constantine, K. L., Friedrichs, M. S., Wittekind, M., Jamil, H., Chu, C.-H., Parker, R. A., Goldfarb, V., Mueller, L. and Farmer, II, B. T. (1998) Backbone and side chain dynamics of uncomplexed human adipocyte and muscle fatty acid-binding protein. *Biochemistry* **37**, 7965–7980
- 43 Lücke, C., Fushman, D., Ludwig, C., Hamilton, J. A., Sacchettini, J. C. and Rüterjans, H. (1999) A comparative study of the backbone dynamics of two closely related lipid binding proteins: bovine heart fatty acid binding protein and porcine ileal lipid binding protein. *Mol. Cell. Biochem.* **192**, 109–121
- 44 Nicholls, A., Sharp, K. A. and Honig, B. (1991) Protein folding and association: insights from the interfacial and thermodynamic properties of hydrocarbons. *Proteins* **11**, 281–296

Received 11 September 2000/6 November 2000; accepted 13 December 2000